Cement & Concrete Composites 32 (2010) 369–376

Contents lists available at ScienceDirect

Cement & Concrete Composites

journal homepage: www.elsevier.com/locate/cemconcomp

# Viscoelastic nature of calcium silicate hydrate

Rouhollah Alizadeh *, James J. Beaudoin, Laila Raki

*Institute for Research in Construction, National Research Council Canada, Ottawa, Canada*

ARTICLE INFO

*Article history:*
Received 5 January 2010
Received in revised form 24 February 2010
Accepted 25 February 2010
Available online 2 March 2010

*Keywords:*
Stress relaxation
Calcium silicate hydrate (C–S–H)
Portland cement
Time-dependent deformations
Interlayer water
Viscoelastic properties

ABSTRACT

The origin of the time-dependent response of cement-based materials to applied stress has not been clearly resolved. The role of interlayer water in the mechanical behavior of calcium silicate hydrate (C–S–H) is still debated. In order to better understand the pertinent mechanisms, the stress relaxation tests were conducted on thin rectangular beams of compacted synthetic C–S–H powder and hydrated Portland cement subjected to three-point bending. C–S–H specimens of variable composition (C/S = 0.8, 1.2 and 1.5) were prepared at various moisture content levels from saturation to the dry state. A special drying procedure was applied in order to remove the adsorbed and interlayer water incrementally from C–S–H conditioned at 11%RH. It was shown that a significant part of the relaxation at saturation is attributed to the hydrodynamic component associated with the pore water. It was demonstrated that the viscoelastic performance of C–S–H depends considerably on the presence of interlayer water. It was argued that the results support the validity of the theory of sliding of C–S–H sheets as a time-dependent deformation mechanism responsible for the creep and stress relaxation of cement-based materials. This concept was illustrated in a proposed model for the viscoelastic response of C–S–H.



## 1. Introduction

The time-dependent changes in the mechanical properties of concrete have been the subject of extensive research over the past century [1]. In particular, the concrete creep, i.e. the strain induced under sustained loading over time, has received significant attention due to its practical implications. Although numerous studies have been conducted in this regard, the nature of creep phenomena in cement-based systems is still not clearly resolved. There are several hypotheses proposed for the concrete creep that describe possible mechanisms for the temporal deformation of hardened concrete under load [2,3]. None of these theories alone can explain all the experimental observations and it appears that multiple mechanisms may be operative. It is argued that the origin of creep is situated at the micro and nano-level within the capillary space and the calcium silicate hydrate (C–S–H)[1] phase, respectively, referred to as the short-term and long-term creep [4].

The theories on the nature of creep that pertain to the nanostructure of the hydrated cement paste are briefly described. The microprestress-solidification theory implies that the overstressed unstable atomic-scale bonds are locally broken and reformed in the 'hindered' adsorbed water molecule sites (including that in the C–S–H interlayer) [5]. This results in a quasi-dislocation of adjacent particles through a shear slip mechanism (i.e. the sliding of C–S–H sheets [4]) which contributes to the long-term creep. The theory of micro-sliding between the adjacent C–S–H sheets and the change in the orientation of hydroxyl water held on the crystalline surfaces was later argued to be the main contributor to the creep behavior [6]. It was also shown that the removal of interlayer water from the hydrated cement system results in an increase of the creep capacity. Removal of the pore water before applying the load on the specimen, however, decreases the creep of concrete [3,7]. This is consistent with the previous investigations that assign a structural role to the water situated between the layers of C–S–H [8–10]. It was, however, suggested by some researchers that no creep occurs if all the evaporable water is removed from the hydrated system [11–13].

Creep of concrete has also been described in terms of a nanogranular model of C–S–H particles [14–16]. It was suggested that the creep may involve the rearrangement of the C–S–H globules resulting in a tighter local packing, i.e. higher local density. This theory was later modified in Jennings' second generation model for C–S–H (CM-II) to account for the role of large gel pores (LGP) in the creep of C–S–H [17]. It was suggested that the volume of LGP is gradually reduced under stress and that the LGP may collapse due to the rearrangement of particles. The interlayer water (although a feature in the CM-II) was not considered in the explanation of time-dependent deformation of C–S–H. The granular model is, nevertheless, consistent with the Feldman's layered model for C–S–H [9] in that they both propose that the solid volume of C–S–H increases (i.e. tighter local packing) due to creep. It was

* Corresponding author. Tel.: +1 613 993 5117; fax: +1 613 954 5984.
*E-mail address:* aali.alizadeh@nrc.ca (R. Alizadeh).

[1] Cement chemistry nomenclature: C = CaO, S = $SiO_2$ and H = $H_2O$. Hyphens indicate no specific stoichiometry is applied.

0958-9465/$ - see front matter © 2010 Elsevier Ltd. All rights reserved.
doi:10.1016/j.cemconcomp.2010.02.008

postulated in the layered model that new interlayer regions are formed under stress [9,18]. Two types of C–S–H were considered in the granular model and it was proposed that the low density (LD) C–S–H (i.e. packing density) creeps more than the high density (HD) C–S–H in cement paste possibly due to the difference in the porosity levels and not the intrinsic properties of the C–S–H [15]. Another category of C–S–H (ultra high density) was recently identified using a nanoindentation technique and the source of creep was attributed to the particle-to-particle contact of nano-sized C–S–H [19]. The moisture content of the samples, however, was not considered in the discussions. Moreover, it was suggested that the C–S–H exists in compositionally similar forms even though a wide range of cement mixes was used. A similar conclusion was also made that the mechanical properties of C–S–H phases are a sole function of their packing density [20]. The C–S–H creep data obtained from nanoindentation experiments and expressed as a logarithmic function was shown to be only dependent on the packing density of C–S–H. The logarithmic-type behavior of the creep of C–S–H in hydrated cement paste at the nano scale was also confirmed in a separate study but the LD and HD C–S–H phases were not distinguished [21].

It is well-known that the stoichiometry of C–S–H in hydrated cement paste can readily be changed by various parameters such as curing conditions and use of supplementary cementitious materials [22]. It is therefore necessary to establish a relation between the chemistry of C–S–H and its engineering characteristics including time-dependent mechanical properties. Hardened cement paste is not an ideal material for the studies in this regard. The porosity, which has an important role in the mechanical behavior of the porous body of the solid, is obviously influenced by the mix characteristics of the cement paste. Moreover, the chemical properties of C–S–H and additional phases formed in the hydration reactions cannot be easily controlled. The mechanical characterization results therefore cannot be related independently to the stoichiometry of the C–S–H in these systems.

The stress relaxation of cement and concrete, a mechanical property that is closely related to the creep, has rarely been studied mainly due to the experimental limitations [23]. A relatively quick method using three-point bending of thin cement paste beams that was primarily adopted to measure the permeability of hardened cement, was successfully used to separate the main components of the stress relaxation in saturated Portland cement paste; hydrodynamic and viscoelastic [24–27]. The pressure gradients in saturated pores under stress are alleviated through the flow of the fluid causing the hydrodynamic relaxation that diminishes at early times. The internal redistribution of water in the capillary space was identified as a factor responsible for the short-time creep [28]. Water molecules may be re-adsorbed into the fine pore structure of the paste upon unloading [29]. The solid network of the materials undergoes a viscoelastic relaxation that remains active at later times. The three-point bending method was applied in the current work in order to study the stress relaxation behavior of synthetic C–S–H as well as hydrated Portland cement and porous glass.

The synthetic semi-crystalline C–S–H (i.e. C–S–H(I) of variable C/S ratio) was chosen for this study since it has been considered as an appropriate model for the nearly amorphous C–S–H produced in the hydration of Portland cement [10,30]. A solid body of the phase pure C–S–H is, however, required for the investigation of its mechanical performance. The current research utilizes the compaction technique in order to prepare rectangular beams from the powdered materials (synthetic C–S–H of variable stoichiometry) at a controlled porosity level. It should be noted that the synthetic C–S–H is a fully hydrated material and the effect of the hydration of cement during the conventional creep measurements as well as other aging mechanisms [31] are eliminated. The results of the stress relaxation measurement in the compacted C–S–H specimens subjected to a constant strain in a three-point bending set-up at various humidity levels are reported. Samples of hydrated Portland cement and porous glass were also tested for comparison. It is primarily intended to examine the role of the interlayer water in the time-dependent deformation of C–S–H with respect to its chemical composition.

## 2. Method

### 2.1. Materials

C–S–H was synthesized by means of a pozzolanic reaction between amorphous $SiO_2$ and CaO in excess water (water/solid ratio by mass $\approx 10$). Reactive silica (Cab-O-Sil grade M-5, Cabot Corporation) was heated at 110 °C. Calcium oxide was obtained from the calcinations of the reagent grade calcium carbonate (Sigma–Aldrich Company) at 900 °C. All materials were kept in sealed $N_2$ purged bottles until used. Various C–S–H systems were prepared using stoichiometric amounts of CaO and $SiO_2$ resulting in C/S ratios of 0.8, 1.2 and 1.5. Distilled de-aired water was added to the dry mixture of CaO and $SiO_2$ in 1 L HDPE bottles. The bottles were mounted on a rotating rack (at the speed of 16 rpm) and the reaction continued for 180 days. The chemical reaction is nearly completed in the first week, but further time is required in order to obtain a well-ordered crystalline structure. The material produced was filtered after this period and dried under vacuum for 4 days at room temperature. High drying temperatures were avoided during the material preparation since the crystal structure of C–S–H can be altered in extreme drying condition occurring at temperatures above 50 °C [32]. The dried C–S–H powders were stored in nitrogen purged glass vials before experiments. During these steps maximum care was taken to minimize the C–S–H surface carbonation due to the exposure of the material to the $CO_2$ in atmosphere.

Two other sets of samples were prepared for comparison: the cement paste and porous glass. Rectangular prisms ($250 \times 100 \times 12$ mm) were cast from the Portland cement paste (Lafarge Canada type I) at a water/cement ratio of 0.4. The prism was vibrated and stored in a moist curing room for 24 h. It was then demoulded and curing was continued for 2 months in the saturated lime solution. Thin slices ($\sim 1 \times 12 \times 60$ mm) were cut from the cement paste bar using an Isomet diamond saw. Vycor® porous glass plate (thickness = 1.3 mm, surface area = 110 $cm^2/g$, porosity $\approx 28\%$) was cut to give rectangular specimens measuring $12 \times 60$ mm. The length of the specimens was chosen according to the standard requirements of the three-point bending test [33,34]. An over-edge of about 10% of the specimen length was considered on each side from the supports. The length/thickness ratio (about 40) was well above the specified value of eight.

The C–S–H preparations and cement paste slices were conditioned for three weeks in a vacuum desiccator over the vapor pressure of a saturated lithium chloride solution. This provides a relative humidity of about 11% at room temperature which is a desirable base for studying the stoichiometry of C–S–H [35]. There is, theoretically, only a monolayer of adsorbed water on the surface of particles at this specific humidity in addition to the interlayer water. This state was used as the starting condition for most of the experiments in the current work. Additional samples were conditioned over the vapor pressure of water for stress relaxation experiments in the saturated state (100%RH).

Unlike the hardened cement paste that can be cast and cut into various shapes for engineering investigations, it is necessary to prepare solid samples by compacting the fine powder for mechanical measurements of phase pure materials such as calcium hydroxide and synthetic C–S–H [36,37]. The porosity of the sample

can be readily controlled in the compaction technique. The bonds forming between the particles in the compacted sample are essentially similar to those that form during the setting and hardening of cement paste [38,39].

Compacted specimens were prepared from the C–S–H powder conditioned at 11%RH for one month as follows. Two grams of C–S–H powder were compacted in a steel mould consisting of a cylinder and two closely fitting pistons. The plan view of the prepared samples is shown in Fig. 1. The steel mould was first mounted vertically with the bottom piston. The C–S–H powder was then placed in the cylinder. The top piston was then placed in the cylinder and the assembly was mounted in a compression machine. The pressure was increased gradually to a specified value where it was maintained for about 30 s before releasing. The compacted specimen was removed by pressing out the pistons. A specific compaction pressure was applied for each C/S ratio in order to achieve a porosity level of about 30% in the compacted samples where a sufficiently large fraction of the solid material would come into the play and the behavior would better represent that of the C–S–H. More details about the compaction procedure can be found elsewhere [10]. A length of 55.9 mm was cut from the rectangular compact bars to fit the specimen requirements in the stress relaxation instrument. The thickness of the compacted C–S–H samples varied between 0.8 and 1.2 mm depending on the C/S ratio and the compaction pressure. The relatively low thickness allows for decreasing the time to achieve the equilibrium state at various humidity levels and avoiding major moisture gradients that may result in micro-cracking in the test specimens subjected to drying. The compacted samples were kept in a vacuum desiccator at 11%RH. The additional conditioning at this humidity resulted in about 1% mass loss in the samples. It is suggested that the monolayer of water present on the surface of particles before compaction may have moved to 'pore' spaces after the particles come into contact in the compacted sample. Excess water in the pores is then removed during equilibration with 11%RH condition.

### 2.2. Experimental procedure

The starting humidity condition for the compacted C–S–H specimens as previously mentioned was obtained in equilibrium with 11%RH. Saturated samples were prepared by conditioning the compacted specimens at 100%RH. Lower humidity levels were achieved by the removal of water from 11%RH conditioned samples through the application of a combination of vacuum and heat. The initial drying increments were conducted at room temperature using only vacuum in a special glass cell. The temperature was gradually increased using the voltage adjustment (with a VARIAC W5MT3) on the heating mantle wrapped around the glass cell for higher mass loss levels in the samples. The temperature inside the cell under vacuum had been previously calibrated for the voltage. In order to minimize altering the C–S–H structure, the drying temperature for most increments of mass loss was kept below 50 °C while increasing the duration of vacuum. The drying temperature never exceeded 110 °C at mass loss increments (up to 10%) approaching the dry state. These humidity levels can be considered as quasi-equilibrium states considering the substantial amount of time spent on the water removal at each increment. It takes about one to two weeks to collect the whole set of data for each sample. It is important to increase the temperature and vacuum duration between various mass loss increments very gradually in order to avoid moisture gradients that may cause micro-cracking in the specimens.

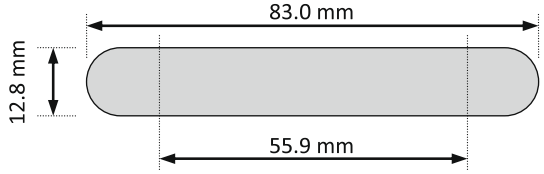


**Fig. 1.** The plan view of the compacted C–S–H samples. The middle part was cut to obtain the specimens for stress relaxation experiments. The cement paste and porous glass samples had similar dimensions. The average thickness of all samples was about 1 mm.

The stress relaxation test was conducted at each increment of water removal using a Rheometrics RSA III instrument. The rectangular samples were wrapped with cellophane film after drying in order to keep the humidity level constant during the test. The elasticity of cellophane wrap was negligible in comparison with that for the samples. This was examined using a steel plate with and without cellophane wrap. Moreover, there was no mass change in the specimens covered with the cellophane film during the relaxation test. The three-point bending method was used for the stress relaxation studies. A static load of 10 g followed by a maximum strain of 0.02% was applied at the middle span of the samples. This sufficiently low strain level resulted in an applied stress below 2 MPa and did not cause any micro-cracking as verified through microscopic analysis. The load required to keep the strain constant was monitored up to four hours. The change in the corresponding stress was recorded by the computer. It should be mentioned that no indentation was observed on the surface of the samples caused by the supports since the contact line is wide enough on the flat specimens to distribute the load. Therefore, no correction was required in the deflection of the rectangular samples. The Hertizian indentation, however, has previously been observed in cement rods [24]. A circular cross-section essentially provides a point contact with the support and high localized stress results in measurable indentation. A separate sample was prepared and tested for each humidity level and drying state, as the stress relaxation is only partially recoverable and the sample cannot be reused for the experiments in the other humidity levels. Several C–S–H samples were tested for the same humidity level in order to obtain reliable data when certainty was not clear.

## 3. Results and discussion

The results for the stress values ($\sigma_t$) versus time were normalized to the initial stress ($\sigma_0$) recorded after the application of the strain. The applied strain increased gradually from zero and reached the maximum constant value after about 0.1 s, at which time the maximum stress value was obtained. The data for up to about 0.6 s is relatively noisy. This shows the equilibrium state of loading is not instant and there are some parameters affecting this period before achieving a more stable state of stress. The general trend during this period, however, follows that of the later times. Some fluctuations were observed in the stress relaxation of a few samples which might be due to the experimental limitations associated with the instrument.

### 3.1. Porous glass

Porous Vycor® glass has been extensively used as a model system in the study of the cement-based materials [40]. The stress relaxation curves for the porous glass samples conditioned at 11% and 100% RH are shown in Fig. 2. A dry sample was also prepared from the 11%RH conditioned porous glass by applying vacuum at 110 °C for 3 h. This resulted in about a 2% mass loss (ML). The total stress relaxation of porous glass samples is not large. The curves show, as expected, a decrease in the stress required in order to maintain the constant strain. The rate and the extent

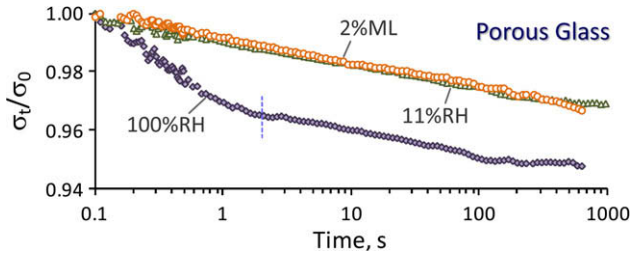


**Fig. 2.** Stress relaxation curves of Vycor® porous glass at various humidity levels. ML = mass loss (% from 11%RH condition). The dashed vertical line indicates the location of inflection point in the 100%RH curve.

of this decrease are dependent on the moisture content of the specimen. The maximum relaxation of about 5% is observed in the saturated specimen after about $10^3$ s. The stress relaxation curve at this humidity level consists of two parts separated by an inflection point at about 2 s (indicated by a dashed vertical line on the curve). This observation is consistent with a previous study on porous glass [41]. The first part of the stress relaxation is due to the release of pore water pressure (hydrodynamic). The second part is attributed to the solid body of the glass that exhibits a relatively small viscoelastic behavior.

There is ideally only a monolayer of water present on the surface of the solid body of the porous glass at the 11%RH condition [34]. The porous glass sample at this relative humidity, therefore, does not exhibit hydrodynamic relaxation associated with the pore water and it only shows a gradual decrease in the stress at a constant rate (in log scale). The dry specimen (2% mass loss from 11%RH) demonstrates a very similar relaxation behavior to that of the 11%RH conditioned sample. It is also noted that the rate of decrease in the stress after the inflection point for the saturated sample is similar to that for the specimens at the 11%RH and dry conditions. It appears that the viscoelastic response of porous glass is not dependent on its moisture content. These observations were repeatedly made and may suggest that the monolayer of water does not have a major contribution to the stress relaxation of porous glass. It is also possible that the effect is so small that it can not be captured accurately by the current experimental set-up. The latter seems more plausible as it has been suggested that the water molecules (available at 11%RH) attack the strained siloxane bonds of porous glass resulting in a viscoelastic relaxation [41].

### 3.2. C–S–H

The stress relaxation curves of compacted samples of synthetic C–S–H (C/S ratios = 0.8, 1.2 and 1.5) at various humidity levels are shown in Fig. 3. In all samples, the saturated specimen (100%RH) experiences a significantly higher total stress relaxation at the initial times. The shape of the curve and the rate of decrease in the stress are different at this moisture content from those at 11%RH and below. This difference is mainly attributed to the presence of hydrodynamic component of the stress relaxation that is active at initial times in the saturated samples. This part is eliminated following the release of the pore water pressure after about 20 s at which time an inflection occurs in the stress relaxation curve in all the saturated C–S–H samples. The observation of the similar time for the end of hydrodynamic relaxation suggests that the C–S–H specimens have a comparable pore structure. The higher stress relaxation in the saturated samples may also be due to a contribution to shear deformation in the C–S–H structure resulting from local fluctuations in the deviatoric stress induced by pore water pressure. As mentioned, all specimens had a similar total porosity of about 30%. The remainder of the relaxation behavior is attributed to the viscoelastic component of the C–S–H phase (i.e. associated with the deformation of the solid body of the specimens).

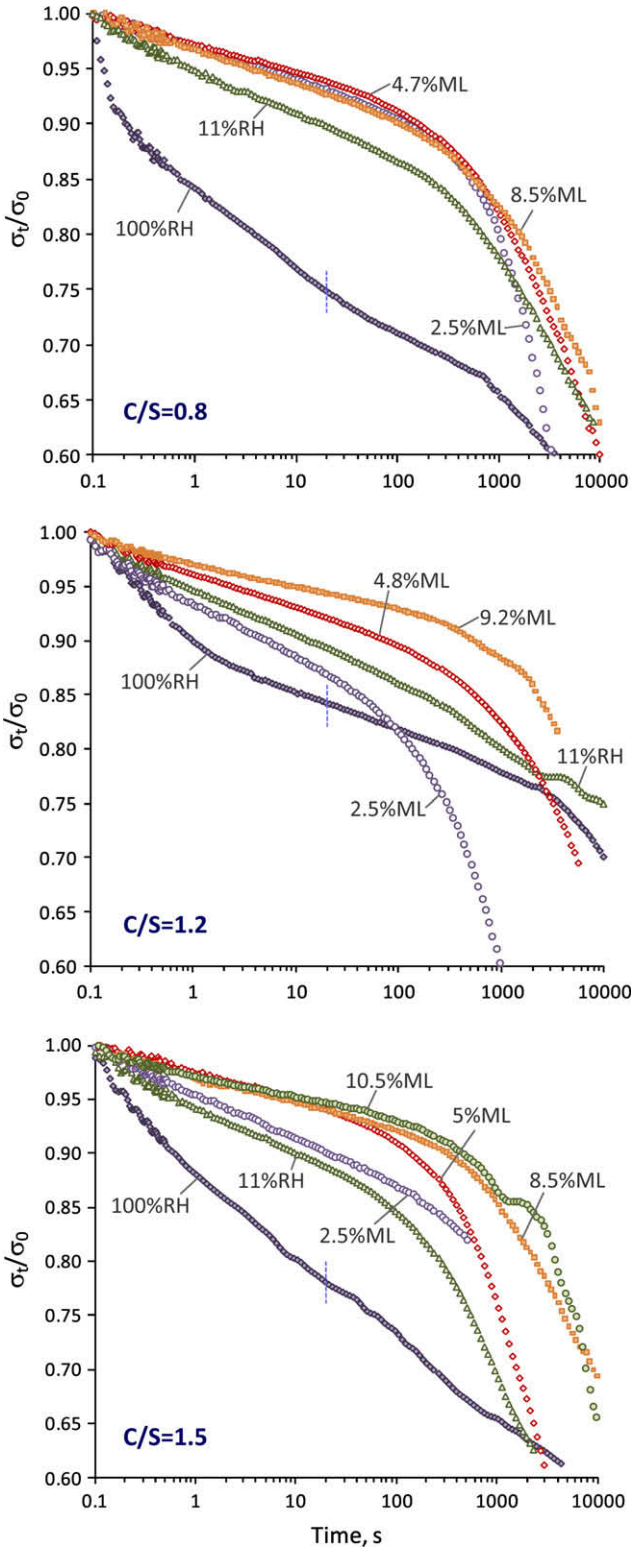


**Fig. 3.** Stress relaxation curves for the C–S–H samples of variable stoichiometries at various moisture contents. The compacted specimens were prepared from the C–S–H powder conditioned at 11%RH. ML = mass loss (% from 11%RH condition). The dashed vertical line indicates the location of inflection point in the 100%RH curve.

The other curves (at 11%RH and lower moisture contents) for all C–S–H samples show a different relaxation response than that of

the 100%RH condition. The hydrodynamic component, that results in a remarkable alleviation of the stress at the initial times for the saturated samples, appears to be eliminated in these specimens. This is due to the absence of 'pore water' at such low humidity levels. The deformation of the pore structure under stress does not lead to an increase in the pore water pressure as in the saturated condition. The stress is directly transferred to the solid structure of the compacted C–S–H agglomorates. A dominant viscoelastic response is therefore observed in all the 'dry' specimens from the beginning as soon as the stress is applied. It is however likely that water may exist in entrapped spaces. The water at these structural locations can not be readily removed and may slightly contribute to a negligible hydrodynamic relaxation that would be dissipated at a prolonged period of time compared to that for the pore water. Some of the relaxation curves in the 'dry' state (11%RH and below) contain a subtle concave-up portion at the beginning within the first 100 s. This is likely associated with a hydrodynamic component other than that related to the pore water.

It is noted (in Fig. 3) that the drying of specimens conditioned at 11%RH changes the viscoelastic response of the C–S–H generally resulting in a lower stress relaxation at initial times more noticeably in the C/S = 1.2 and 1.5 samples. At later times the relaxation curves may intercept with each other resulting in different total stress relaxation values not fully correlated with the mass loss level. The water molecules removed through drying of the 11%RH equilibrated samples are essentially located between the sheets of the layered synthetic C–S–H. It is, therefore, suggested that the interlayer water has a considerable role in the time-dependent viscoelastic deformation of the C–S–H. In order to examine this, a few 11%RH conditioned compacted C–S–H samples were completely dried and equilibrated again to the 11%RH condition. The first drying results in the removal of the interlayer water but water molecules cannot fully enter the interlayer region on the re-wetting at 11%RH [42]. The stress relaxation of the C–S–H specimens subjected to this regime (not shown) was significantly lower than that in the control specimens (originally conditioned at 11%RH). It is suggested accordingly that the presence of the interlayer water facilitates the time-dependant deformation of C–S–H under load. The mechanism of viscoelastic behavior of C–S–H may therefore be attributable to the sliding of the C–S–H sheets as hypothesized before [4,6]. In order to verify this, X-ray diffraction was conducted before and after the stress relaxation test on representative C–S–H samples at various moisture content levels. Synthetic C–S–H has a basal spacing reflection ($d_{002}$) unlike the C–S–H in the hydrated Portland cement. The test results (not shown), however, did not suggest any noticeable change in the location ($2\theta$) and the intensity of the 002 basal spacing peak of the compacted C–S–H samples subjected to stress. Theoretically, it is possible that the layers slide parallel to each other without affecting the reflection of the X-ray. The XRD investigation also suggests that the C–S–H layers are not likely compressed under stress. Analytical methods for short-range order investigation such as NMR might be able to provide more evidence in this regard if mechanisms such as breaking of silicate and hydrogen bonds (consistent with previous theories [5]) apply.

It has been previously shown that the mechanical properties of C–S–H systems are significantly influenced by the interlayer water [10]. It was also suggested that the removal of water molecules from the interlayer region may also lead to nanostructural interactions primarily related to the silicate tetrahedra and the calcium ions situated between the C–S–H sheets. These changes modify the mechanical response of C–S–H at various steps resulting in an oscillatory dynamic mechanical behavior. This might be responsible for some of the inconsistencies in the order of the stress relaxation curves versus mass loss on drying of C–S–H below 11%RH. It is also noticed that the stress relaxation of the C–S–H samples having the lowest C/S ratio (C/S = 0.8) does not vary substantially as the interlayer water is removed. It appears that for this C/S ratio all the curves corresponding to the moisture contents below 11%RH are qualitatively similar. At higher C/S ratios (1.2 and 1.5), however, the stress relaxation curves are well-separated for various increments of drying. This may suggest that interlayer water has a more significant structural role in high C/S ratio C–S–H. The difference in the mechanical properties of C–S–H samples separated at a C/S ratio of about 1.1 has been previously observed [10].

In order to compare the viscoelastic behavior of C–S–H of variable compositions together and also between the 'dry' states and the saturated condition, it is necessary to separate the hydrodynamic and viscoelastic components of the stress relaxation curve for samples at 100%RH. Extensive work by Scherer's group at Princeton has led to developing and solving the stress relaxation equations for the hydrated Portland cement [23–26]. These equations are applicable only at the saturated state. An analytical solution for the load ($W$, which is directly related to the stress) as a function of time for a rectangular cross section beam can be expressed as:

$$W(t) = W(0)R(t)\Psi_{VE} \tag{1}$$

where $R(t)$ is the hydrodynamic and $\Psi_{VE}(t)$ is the viscoelastic relaxation function. The hydrodynamic component can be described by the following equation:

$$R(t) = 1 - A + AS_1(\theta)S_2(\kappa\theta) \tag{2}$$

where $A$ is the material parameter, $S_1$ and $S_2$ are functions reflecting the rate of the hydrodynamic relaxation, $\theta$ is the reduced time ($\theta = t/\tau_R$) and $\kappa$ is the square of the aspect ratio ($\kappa = a^2/b^2$, for a sample with thickness $2a$ and width $2b$). The $S$ functions that are roots of the Bessel function are given approximately by:

$$\begin{aligned} S_1(\theta) &\approx \exp\left[-\left(\tfrac{6}{\sqrt{\pi}}\right)\left(\tfrac{\theta^{0.5}-\theta^{2.5}}{1-\theta^{0.551}}\right)\right] \\ S_2(\theta) &\approx \exp\left[-\left(\tfrac{2}{\sqrt{\pi}}\right)\left(\tfrac{\theta^{0.5}-\theta^{2.094}}{1-\theta^{0.670}}\right)\right] \end{aligned} \tag{3}$$

The viscoelastic part of the relaxation can be described by the following expression:

$$\Psi_{VE}(t) = \frac{\exp\left[-\left(\frac{t}{\tau_2}\right)^{b_2}\right]}{1 - \exp\left[-\left(\frac{t}{\tau_1}\right)^{b_1}\right] + \exp\left[-\left(\frac{t}{\tau_2}\right)^{b_2}\right]} \tag{4}$$

where $\tau_1$ and $\tau_2$ are viscoelastic relaxation times. Through the curve fitting of the Eq. (1) to the experimental data of the load (or stress) versus time, the free parameters are obtained. These include theoretical load at zero time ($W(0)$), material property ($A$), hydrodynamic relaxation time ($\tau_R$), viscoelastic relaxation times ($\tau_1$ and $\tau_2$) and their powers ($b_1$ and $b_2$). The two components of the stress relaxation can then be easily separated. As mentioned, the data for the stress ($\sigma(t)$ can be used in which case the free parameter of $\sigma(0)$ is used instead of $W(0)$.

The extracted viscoelastic component of the C–S–H samples conditioned at 100%RH (shown in Fig. 4) was obtained by substituting the curve-fitted parameters in the Eq. (4). It is observed that the total viscoelastic relaxation of the saturated specimen ($\sigma(t)/\sigma$ (0) at $10^4$ s), for the same C/S ratio, is less than the total stress relaxation of most of the specimens dried below 11%RH. This could also be concluded indirectly from the unprocessed stress relaxation results (Fig. 3) where the stress relaxation curve of the 100%RH conditioned specimen is intercepted by almost all the other curves for samples having lower moisture contents. This may suggest that the removal of interlayer water modifies the viscoelastic nature of the C–S–H and results in an increase of the total stress relaxation. The increase in the creep compliance (analogous to the stress relaxation) upon drying has been

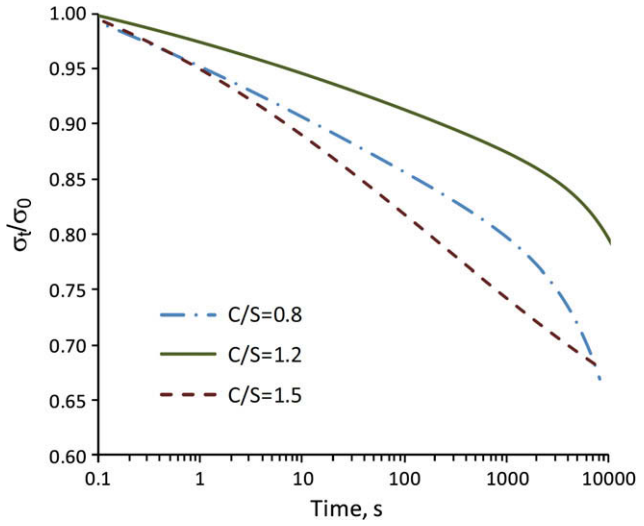


**Fig. 4.** The viscoelastic component of the stress relaxation extracted through curve fitting of the data for the 100%RH conditioned C–S–H samples having various C/S ratios.

previously reported for the Portland cement paste [6]. It should also be noted that the 100%RH curve for porous glass (Fig. 2) does not intercept with the curves for samples at 11%RH and dried conditions. The viscoelastic component of the porous glass appears to be independent of the moisture content (essentially related to the water adsorbed on the surface of solid phase and that in the pores). This observation supports the suggestion that the variations in the viscoelastic properties of C–S–H are attributable to the role of interlayer water. The difference in the surface energy of the C–S–H (compared between the 100%RH and the 'dried' states) might be additionally responsible for partial changes in the viscoelastic response of the C–S–H. It is not clear from the results of the current study if the viscoelasticity of the C–S–H is dependent on its chemical composition. It would be necessary to examine a larger number of specimens having a wider range of C/S ratio to confirm this. The storage modulus ($E'$) and internal friction ($\tan\delta$) obtained through a dynamic mechanical analysis of C–S–H were previously shown to be dependent on the C/S ratio of the C–S–H [10].

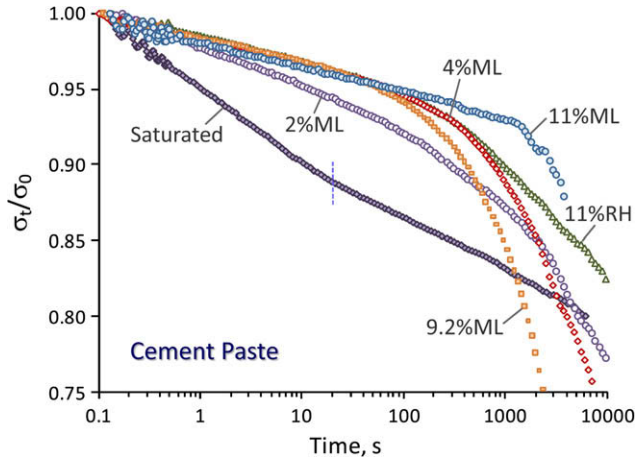


**Fig. 5.** Stress relaxation of the Portland cement paste ($w/c = 0.4$) at various humidity levels. ML = mass loss (% from 11%RH condition). The dashed vertical line indicates the location of inflection point in the relaxation curve for the saturated sample.

### 3.3. Hydrated Portland cement

The stress relaxation curves of the Portland cement paste ($w/c = 0.4$) are shown in Fig. 5. The general trend in terms of the order of the curves for the samples in the saturated state to the 11%RH condition and below seems to be similar to those for the synthetic C–S–H. The saturated cement paste exhibits a distinct behavior, as mentioned for the compacted C–S–H samples, due to the hydrodynamic component of the stress relaxation. The inflection point in the curve seems to occur at about 20 s, analogous to that for the synthetic C–S–H, but much earlier than the values previously reported for the stress relaxation of the cement paste [23–26]. This difference is possibly due the fact that the hydrodynamic relaxation time is directly related to the square of the thickness [26]. The average thickness of the rectangular cement paste specimens tested in the current study was about 1 mm. In comparison to the results for the synthetic C–S–H (Fig. 3), the cement paste exhibits a noticeably lower stress relaxation. This is likely due to the difference between the degree of crystallinity of the C–S–H in the cement paste and that in the synthetic C–S–H. The relatively well-ordered and semi-crystalline structure of the synthetic C–S–H may provide more sliding sites (analogous to "creep sites") contributing to the stress relaxation. It is suggested that these sites are associated with the interlayer region of C–S–H. Comparison of the stress relaxation curves at 11%RH and subsequent incremental drying does not provide conclusive information related to the removal of water but is indicative of the role of interlayer water in the stress relaxation of cement paste. It should also be noted that in cement paste, the stress is gradually redistributed from C–S–H to non-creeping components such as unhydrated cement and calcium hydroxide [43]. This in turn decreases the total viscoelastic deformation of Portland cement paste in comparison to that in the phase pure C–S–H. It is well-known that the C–S–H in the hydrated cement paste is a nearly amorphous material [29]. The silicate structure is modified by the incorporation of other elements such as aluminum. Several types of cations may exist in the interlayer region. These parameters increase the complexity of the C–S–H structure and are likely to be responsible for the variations different from those for the synthetic C–S–H in the stress relaxation upon drying. It is, however, clear that the relaxation curves of 'dry' specimens intercept with the curve of the saturated one (similar to the observation for synthetic C–S–H in Fig. 3). This may be indicative of an increase in the viscoelastic deformation of C–S–H in cement paste when interlayer water is removed, analogous to the results obtained for the synthetic C–S–H.

It is noted that there is a considerable stress relaxation in the dry cement paste (Fig. 5) and C–S–H samples (Fig. 3) after the removal of final increments of water (about 10% mass loss from the 11%RH condition achieved by 24 h vacuum drying at 110 °C). This may imply that even the completely dry solid structure of the C–S–H undergoes time-dependent deformations under load. Although water has a significant contribution to the stress relaxation of the C–S–H, it appears that the stress relaxation does occur in the dry state. This is contradictory to some research that suggests there is no creep behavior in the cement paste if the evaporable water is removed [11–13].

## 4. A model for stress relaxation and creep

The stress relaxation of C–S–H samples consists of hydrodynamic and viscoelastic components. The hydrodynamic component depends on the pore structure characteristics of the sample and the saturation level of the pores. The viscoelastic component of the stress relaxation appears to be dependent on the nanostructural features of the C–S–H. Interlayer water is suggested to contribute

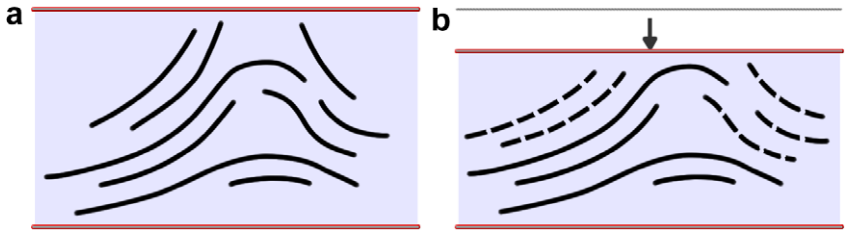


**Fig. 6.** Proposed model for the viscoelastic behavior of the C–S–H. (a): C–S–H layers are shown by solid lines. The nanostructural features are based on the Feldman–Sereda model for C–S–H [44]. (b): The time-dependent deformation of C–S–H under load through the translation and sliding of the layers (shown by dashed lines).

significantly to the viscoelasticity of the C–S–H and thus its time-dependent mechanical properties such as stress relaxation and creep. Several models have been proposed for the creep of concrete [2,3]. A combination of mechanisms appear to account for the temporal deformation of cement-based materials. The following model is proposed based on the ideas advanced in the current study with a focus on the role of interlayer water.

The schematic in Fig. 6a presents a very simplified model of the C–S–H. The agglomerates of layered C–S–H are formed from the stacking of several sheets of C–S–H having nanostructural features similar to those proposed by Feldman and Sereda [44]. A monolayer of water is ideally situated in the interlayer region in addition to the $OH^-$ groups and $Ca^{2+}$ ions. Under load (Fig. 6b) the stress is applied to the solid pore-network. The deformation of the pore-network results in an increase of the water pressure in the pores which is alleviated later by the flow of water. This accounts for the hydrodynamic relaxation. There is an elastic deformation in the C–S–H solid phase. In addition, it is suggested that under stress the C–S–H agglomerates exhibit a viscoelastic deformation over time. The C–S–H sheets translate with respect to each other. A progressive breaking and formation of hydroxyl bonds in the interlayer region may also be postulated [5,6]. The sliding of the C–S–H layers is proposed as the mechanism responsible for the viscoelastic behavior of C–S–H. This, in nature, is similar to the concept of the rearrangement of C–S–H globules [16] with creep sites situated at the "particle-to-particle" contacts [19] and may result in a tighter packing of the C–S–H agglomerates. The nanogranular model for C–S–H, however, can not explain the variations in the viscoelastic response of C–S–H at various interlayer moisture contents unless a structural role is assigned to the interlayer water. Water molecules "reinforce" the C–S–H sheets. It is suggested that their removal increases the total stress relaxation of the C–S–H. Viscoelasticity of C–S–H is readily modified by the change in the moisture content associated with the interlayer water. Cross-linking of silicate tetrahedra and the interaction of calcium ions with the silicate chain at various humidity levels are likely to be responsible for some of the inconsistent variations of the stress relaxation upon the removal of interlayer water. Further studies elucidating the effect of these parameters on the time-dependent deformation of cement-based materials would be revealing. The development of a more comprehensive model that can explain all the experimental observations is subject to advanced corroborative research utilizing analytical tools such as NMR.

## 5. Concluding remarks

The stress relaxation behavior of phase pure C–S–H (C/S = 0.8, 1.2 and 1.5), hydrated Portland cement and porous glass was studied using a three-point bending method. The samples were tested at various moisture contents obtained by conditioning at 100%RH and 11%RH as well as removing water in several drying increments from the 11%RH condition.

It was shown that the hydrodynamic component (present in the 100%RH condition) has a significant contribution to the stress relaxation of C–S–H at the initial times (up to 20 s). At later times when the pore water pressure is alleviated, the viscoelastic part of the stress relaxation becomes dominant. The stress relaxation curves of the samples at 11%RH and lower humidity levels apparently do not exhibit a hydrodynamic relaxation. They exhibit primarily viscoelastic behavior. The viscoelastic component of porous glass is similar at all humidity levels and does not appear to be dependent on the moisture content. In cement-based systems, however, the viscoelastic response of C–S–H is altered (generally in the form of a relative decrease at the initial times and an increase at later times) as the water is removed from the interlayer region. The total stress relaxation of most 'dry' specimens (i.e. conditioned at 11%RH and below) is greater than that for the samples conditioned at 100%RH in both C–S–H and cement paste shown in Figs. 3 and 5, respectively. This is not the case for porous glass. It is suggested that the interlayer water plays an important role in the time-dependent deformation of cement-based materials. The viscoelastic behavior of C–S–H is attributed to the sliding of the C–S–H sheets which results in the deformation of C–S–H agglomerates under stress. The siloxane bonds may be broken and reformed due to the translation of the C–S–H layers. Removal of water from interlayer spaces modifies the viscoelastic behavior of C–S–H resulting in a higher total stress relaxation compared to that for the saturated conditions. Understanding the details of the sliding mechanism of C–S–H layers possibly taking into account the interaction of silicate tetrahedra and cations in the interlayer region at various moisture contents should benefit from further study utilizing methods such as NMR. An investigation of the irreversible creep and stress relaxation in synthetic layered C–S–H systems at various moisture contents would provide additional insight into the nanostructural aspects of the time-dependent deformations in cement-based materials.

## Acknowledgements

The authors would like to acknowledge the helpful discussions with Professor George W. Scherer at Princeton University and the financial support through an NSERC Discovery Grant.

## References

[1] Hatt WK. Notes on the effect of time element in loading reinforced concrete beams. Proc Am Soc Test Mater 1907;7:421–33.
[2] Neville AM. Creep of concrete: plain, reinforced, and prestressed. Amsterdam: North-Holland Publishing Company; 1970. p. 622.
[3] Neville AM, Dilger W, Brooks JJ. Creep of plain and structural concrete. London: Construction Press, Longman Group; 1983. p. 361.
[4] Ulm F-J, Le Maou F, Boulay C. Creep and shrinkage coupling: new review of some evidence. Revue Française de Génie Civil 1999;3:21–37.
[5] Bažant ZP, Hauggaard AB, Baweja S, Ulm F-J. Microprestress-solidification theory for concrete creep. I: aging and drying effects. J Eng Mech 1997;123(11):1188–94.
[6] Tamtsia BT, Beaudoin JJ. Basic creep of hardened cement paste – a re-examination of the role of water. Cem Concr Res 2000;30:1465–75.

[7] Tamtsia BT, Beaudoin JJ. Effect of solvent exchange on length change and creep of D-dried hydrated $C_3S$ paste. Adv Cem Res 2001;13(1):1–9.
[8] Feldman RF. Factors affecting the Young's modulus – porosity relation of hydrated Portland cement compacts. Cem Concr Res 1972;2(4):375–86.
[9] Feldman RF. Mechanism of creep of hydrated Portland cement paste. Cem Concr Res 1972;2:521–40.
[10] Alizadeh R. Nanostructure and engineering properties of basic and modified calcium-silicate-hydrate systems. Ph.D. thesis, Department of Civil Engineering, University of Ottawa; 2009, p. 231.
[11] Glucklich J, Ishai O. Creep mechanism in cement mortar. J Am Concr Inst 1962;59(7):923–48.
[12] Mullen WG, Dolch WL. Creep of Portland cement paste. Proc Am Soc Test Mater 1964;64:1146–71.
[13] Brown NH, Hope BB. The creep of hydrated cement paste. Cem Concr Res 1976;6(4):475–86.
[14] Thomas JJ, Jennings HM. Chemical aging and the colloidal structure of the C–S–H gel: implications for creep and shrinkage. In: Ulm F-J et al., editors. Proceedings of the 6th international conference on creep, shrinkage and durability mechanics of concrete and other quasi-brittle materials. Cambridge (MA): Elsevier; 2001. p. 33–8.
[15] Jennings HM, Thomas JJ, Gevrenov JS, Constantinides G, Ulm F-J. Nanostructure of C–S–H gel in cement paste as a function of curing conditions and relative humidity. In: Pijaudier-Cabot G et al., editors. Proceedings of the 7th international conference on creep, shrinkage and durability of concrete and concrete structures hermes science. France: Nantes; 2005. p. 19–37.
[16] Jennings HM, Thomas JJ, Vlahinić I. Can nano-models lead to improved concrete? Materials science as the intersection of chemistry and mechanics. In: Tanabe T et al., editors. Proceedings of the 8th international conference on creep, shrinkage and durability of concrete and concrete structures. Ise-Shima, Japan: CRC Press; 2008. p. 11–23.
[17] Jennings HM. Refinements to colloid model of C–S–H in cement: CM-II. Cem Concr Res 2008;38:275–89.
[18] Feldman RF, Beaudoin JJ. Effect of applied stress on the helium inflow characteristics of hydrated Portland cement. Cem Concr Res 1983;13:470–6.
[19] Vandamme M, Ulm F-J. Nanogranular origin of concrete creep. Proc Nat Acad Sci 2009;106:10552–10-557.
[20] Vandamme M. The nanogranular origin of concrete creep: a nanoindentation investigation of microstructure and fundamental properties of calcium–silicate–hydrates. Ph.D. Thesis, Massachusetts Institute of Technology, Dept. of Civil and Environmental Engineering; 2008. p. 366. <http://hdl.handle.net/1721.1/43906>.
[21] Pichler Ch, Lackner R. Identification of logarithmic-type creep of calcium–silicate–hydrates by means of nanoindenation. Strain 2009;45:17–25.
[22] Taylor HFW. Cement chemistry. 2nd ed. Thomas Telford Publishing; 1997. p. 459.
[23] Hansen TC. Estimating stress relaxation from creep data. Mater Res Stand 1964;4(1):12–4.
[24] Vichit-Vadakan W, Scherer GW. Beam-bending method for permeability and creep characterization of cement paste and mortar. In: Ulm F-J et al., editors. Proceedings of the 6th international conference on creep, shrinkage and durability mechanics of concrete and other quasi-brittle materials. Cambridge (MA): Elsevier; 2001. p. 27–32.
[25] Vichit-Vadakan W, Scherer GW. Measuring permeability of rigid materials by a beam-bending method: III, cement paste. J Am Ceram Soc 2002;85(6):1537–44.
[26] Vichit-Vadakan W, Scherer GW. Measuring permeability and stress relaxation of young cement paste by beam bending. CemConcr Res 2003;33:1925–32.
[27] Valenza II J, Scherer GW. Measuring permeability of rigid materials by beam-bending method: V, isotropic rectangular plates of cement paste. J Am Ceram Soc 2004;87(10):1927–31.
[28] Sellevold EJ, Richards CW. Short-time creep transition for hardened cement paste. J Am Ceram Soc 1972;55(6):284–9.
[29] Beaudoin JJ, Tamtsia BT. Early age strain recovery of hardened cement paste – microstructural factors. Adv Cem Res 2003;15(2):51–6.
[30] Alizadeh R, Beaudoin JJ, Raki L. C–S–H (I) – a nanostructural model for the removal of water from hydrated cement Paste? J Am Ceram Soc 2007;90(2):670–2.
[31] Grasley ZC, Lange DA. Constitutive modeling of the aging viscoelastic properties of Portland cement paste. Mech Time-Depend Mater 2007;11:175–98.
[32] Mitchell L, Alizadeh R, Whitfield P, Beaudoin JJ. Phases changes in semi-crystalline synthetic calcium–silicate–hydrate, submitted for publication.
[33] ASTM D 5023-01. Standard test method for plastics: dynamic mechanical properties: in flexure (three point bending). Am Soc Test Mater.
[34] ISO 6721-5. Plastics-determination of dynamic mechanical properties-part 5: flexural vibration-non-resonance method. Int Organ Stand.
[35] Feldman RF, Ramachandran VS. A study of the state of water and stoichiometry of bottle-hydrated $Ca_3SiO_5$. Cem Concr Res 1974;4(2):155–66.
[36] Sereda PJ, Feldman RF. Compacts of powdered material as porous bodies for use in sorption studies. J Appl Chem 1963;13:150–8.
[37] Beaudoin JJ. Comparison of mechanical properties of compacted calcium hydroxide and Portland cement paste systems. Cem Concr Res 1983;13:319–24.
[38] Soroka I, Sereda PJ. The structure of cement-stone and the use of compacts as structural models. In: 5th international symposium on the chemistry of cement. Tokyo; 1968. p. 67–73.
[39] Sereda PJ, Feldman RF, Swenson EG. Effect of sorbed water on some mechanical properties of hydrated Portland cement pastes and compacts. Highway Research Board. Special Report; 1966; 90: 58–73.
[40] Ramachandran VS, Feldman RF, Beaudoin JJ. Concrete science. London (UK): Heydon & Son Ltd.; 1981. p. 427.
[41] Vichit-Vadakan W, Scherer GW. Measuring permeability of rigid materials by a beam-bending method: II, porous glass. J Am Ceram Soc 2000;83(9):2240–5.
[42] Feldman RF. Sorption and length-change scanning isotherms of methanol and water on hydrated Portland cement. In: Proceedings of the 5th international symposium on the chemistry of cement, vol. 3. Tokyo, Japan; 1968. p. 53–66.
[43] Šmilauer V, Bažant ZP. Identification of viscoelastic C–S–H behavior in mature cement paste by FFT-based homogenization method. Cem Concr Res 2010;40(2):197–207.
[44] Feldman RF, Sereda PJ. A model for hydrated Portland cement paste as deduced from sorption-length change and mechanical properties. Matériaux et Construction 1968;1(6):509–20.